A Lagrangian ensemble model of *Calanus finmarchicus* coupled with a 1-D ecosystem model

FRANÇOIS CARLOTTI[1,*] AND KARL-ULRICH WOLF[2]

[1] *Université P. et M. Curie (Paris VI); C.N.R.S.-I.N.S.U.; ESA 7076, Station Zoologique, B.P. 28, F-06230 Villefranche-sur-Mer, France*
[2] *Forschungszentrum Jülich, PT BEO, Seestr. 15, 18119 Warnemünde, Germany*

ABSTRACT

A population dynamics model of *Calanus finmarchicus* based on Lagrangian particles has been coupled with a 1-D ecosystem model. Each of the particles represents a variable number of copepods which experience the same fate. Therefore all copepods of a single particle represent a cohort and are characterized by a common set of individual properties such as age, development-stage, depth, structural weight (length), lipid pool or food satiation. The physical environment is parameterized by a 1-D-water column with a vertical resolution of 1 m and a maximum depth of 800 m. Copepod food supply is provided by an interactive Eulerian NPZD model where Z represents microzooplankton. The model correctly reproduces both the dynamics of the ecosystem and the life history of the copepods in the Norwegian Sea. Simulated results of trajectories of particles in the water column, and of individual growth and stage development were analysed. Results on seasonal abundance, development time, number of generations, depth profiles, and patterns of diurnal and ontogenic migration are compared with field data from OWS India.

Key words: *Calanus finmarchicus*, ecosystem dynamics, IBM models, life-cycle

INTRODUCTION

In order to study zooplankton behaviour, individual based models (IBM) are often used as they are able to represent important properties for coupling individual behaviour and physical processes (DeAngelis and Gross, 1992). They permit trajectories of individuals in current flows, e.g. produced by 3-D models, to be followed and to estimate gain and loss of individuals in particular areas (e.g. Werner *et al.*, 1993; Verdier *et al.*, 1997, Miller *et al.*, 1998). As the swimming behaviour depends on several individual characteristics such as size, shape, weight and development stage, several authors have increased the complexity of their models to simulate growth and development of individuals (e.g. Hinckley *et al.*, 1996; Werner *et al.*, 1993; Miller *et al.*, 1998). The capacity to introduce physiological functions at the level of individuals and to simulate the behaviour of organisms in response to external and internal factors permits the examination of several aspects of the ecology of a population (Batchelder and Miller, 1989; Batchelder and Williams, 1995).

However, the biological and the physical environments are often prescribed as forcing fields. The use of IBM to simulate the dynamic interactions between a dominant zooplankton population and its prey has, to our knowledge, not yet been considered for the following reasons:

- It is still difficult to simulate realistic abundances of individuals which tend to increase during their reproduction phase to uncomputable high numbers.
- The representation of a complete set of known biological and biochemical processes involved in the individual budget requires substantial computing time.
- The studied populations were not expected to have a very strong impact on the food resources, and thus a dynamic relationship between zooplankton and its food was not considered.

In our model, we aim to represent the dynamic impact of *Calanus finmarchicus* grazing on its prey, by building an IBM model of *Calanus* coupled with a 1-D ecosystem model. A similar study was made by Carlotti and Radach (1996), but using a stage-structured

*Correspondence. e-mail: carlotti@ccrv.obs-vlf.fr; Fax: +33 4 76 38 34; Tel.: +33 4 93 76 38 39;
Received for publication 28 April 1998
Accepted for publication 3 August 1998

Eulerian model including age-classes within stages. Their model gives an interesting insight to the role of *Calanus* in ecosystem dynamics and shows the importance of representing cohort development. However, large mesozooplankton organisms cannot be sufficiently represented by a single variable such as is usual in NPZ models. Thus, in areas where mesozooplankton dominates the ecosystem dynamics a better representation of cohort development is necessary. As on the one hand Eulerian models are not able to simulate adequately the individual behaviour of organisms and numerous age-classes, and on the other hand IBMs tend to explode numerically, the Lagrangian Ensemble Method (Woods and Onken, 1982; Barkmann and Woods, 1996) offers a feasible compromise.

By building the present model, we had two objectives. First, to simulate the population dynamics of *Calanus finmarchicus* with a Lagrangian Ensemble model interacting with its environment. Secondly, to re-examine the impact of *Calanus* in the North Atlantic pelagic ecosystem dynamics. We chose to run our model based on data from OWS 'India', at 59°N 19°W, around 400 km south of Iceland. At Station India, the vertical distribution of *Calanus* has been well documented (Williams, 1988; Longhurst and Williams, 1979, 1992). Beside the quality of this comprehensive all-year data set, other ecosystem models (Fasham *et al.*, 1990; Fasham 1993; Fasham *et al.*, 1993) have already been tested for this location. This enables a comparison to be made with Eulerian based models.

MODEL STRUCTURE AND EQUATIONS

Physical frame

The physical environment is represented by a water column of 800 m depth with a vertical resolution of 1 m, a rigid surface and no horizontal advection. The fine gridding enables sufficient vertical resolution for the observed vertical migration of *Calanus finmarchicus*. The seasonal cycle of the mixed layer depth (MLD) is taken from Fasham (1993, see his Fig. 2). The time-step of the model is one hour as the focus here is to investigate the different processes and nonlinear interaction of *Calanus* with the related physical and biological environment. We neglected the diurnal variation of the MLD, although it can influence phytoplankton growth, because we concentrate on *Calanus* which generally feeds during the night when the MLD reaches its diurnal maximum. For numerical integration we used a fourth-order Runge–Kutta routine with step size control.

Figure 1. (a) Observed Mixed Layer Depth (MLD) and (b) simulated temperature profiles, both for Station India.

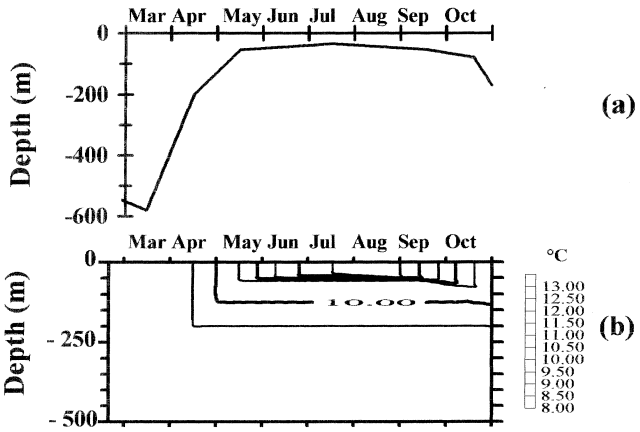

Although the seasonal temperature variation in the biologically active layer is small (9–13°C) and was not parameterized in Fasham's model, we consider an annual cycle in mixed layer (ML) temperature, which is taken from Williams (1988, see his Fig. 8), for the years 1971 and 1974. Below the seasonal thermocline, temperature is considered to stay constant (Fig. 1). Besides turbulent mixing within the ML, all Eulerian variables experience a small 'background' vertical diffusion ($Kz = 0.00001\ m^2\ s^{-1}$).

The sub-surface light field $I(z)$ using 19 spectral bands is calculated after Wolf (1991) as follows:

$$I(z) = I_0 \cdot \sum_{n=1}^{19} R_n(k_n + a \cdot C_{chl}(z)) \cdot dz\ e^{\int_{z=0}^{z'}},$$

where I_0 denotes the actual radiation at the sea surface, R_n and k_n are spectral weighting factors and $C_{chl}(z)$ represents the chorophyll profile as calculated by the ecosystem model.

Ecosystem model

Our Eulerian nitrogen-based ecosystem model (Fig. 2) comprises four state variables: inorganic nitrogen, phytoplankton, microzooplankton and detritus. We suppose that phytoplankton, microzooplankton and detritus have the same C/N ratio. The equations, process formulations and parameter values of the ecosystem model are similar to those presented in Wolf (1991), and are available on request. The nutrient pool represents both nitrate and ammonium. Phytoplankton growth is limited by light and nutrients. The light limitation function is taken from Smith (1936) and nitrate uptake follows Michaelis–Menten kinetics. Phytoplankton is grazed by meso- and micro-

Figure 2. Conceptual flow diagram of the ecosystem model.

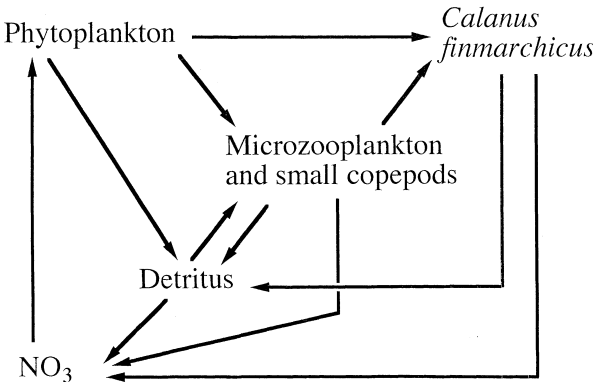

Figure 3. Feeding function on two different prey: principal food (PF) and complementary food (CF).

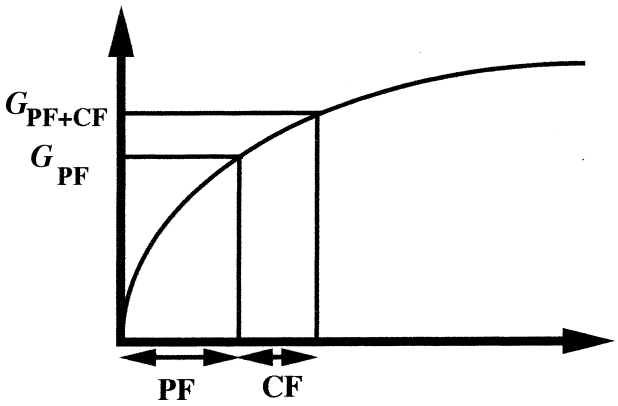

zooplankton. All processes related to mesozooplankton are explained below. The compartment 'microzooplankton' represents animals within a size class between 20 and 200 μm, i.e. the classical microbial food web and small copepods such as *Oithona* sp. Dead phytoplankton, dead microzooplankton, dead *Calanus*, and faecal pellets contribute to the detritus pool while microzooplankton grazing, remineralization and sinking are the loss terms.

Microzooplankton and *Calanus* are able to use two food resources (Fig. 3). We consider that both microzooplankton and *Calanus* graze preferentially on a principal food resource (PF), while the second food resource is called 'complementary food' (CF). For *C. finmarchicus*, we consider phytoplankton as PF, and microzooplankton as CF. Microzooplankton prefer detritus as PF and phytoplankton as CF. The grazing functions, an Ivlev function for microzooplankton and a double linear function for *Calanus*, are used to calculate two grazing values: a first one (G_{PF}) using the PF as single food resource and then a second one (G_{PF+CF}) using the PF plus the CF. The real grazing pressure (G_{CF}) on complementary food is the difference between the two calculated values ($G_{P+CF} - G_P$). It increases inversely with PF abundance. Excretion by microzooplankton and zooplankton, as well as breakdown of detritus contribute to the nutrient pool.

The Lagrangian model of Calanus

In order to model large populations, Woods and Onken (1982) introduced the Lagrangian Ensemble Method where each individual particle comprises a varying number of organisms.

In our model each Lagrangian particle represents a cohort of identical individuals, spawned at the same date and in the same layer. The state variables (characteristic properties) commonly defined for all individuals of a particle are (see also Fig. 4): the depth

Figure 4. Schematic links of a Lagrangian particle with the other components of the ecosystem model.

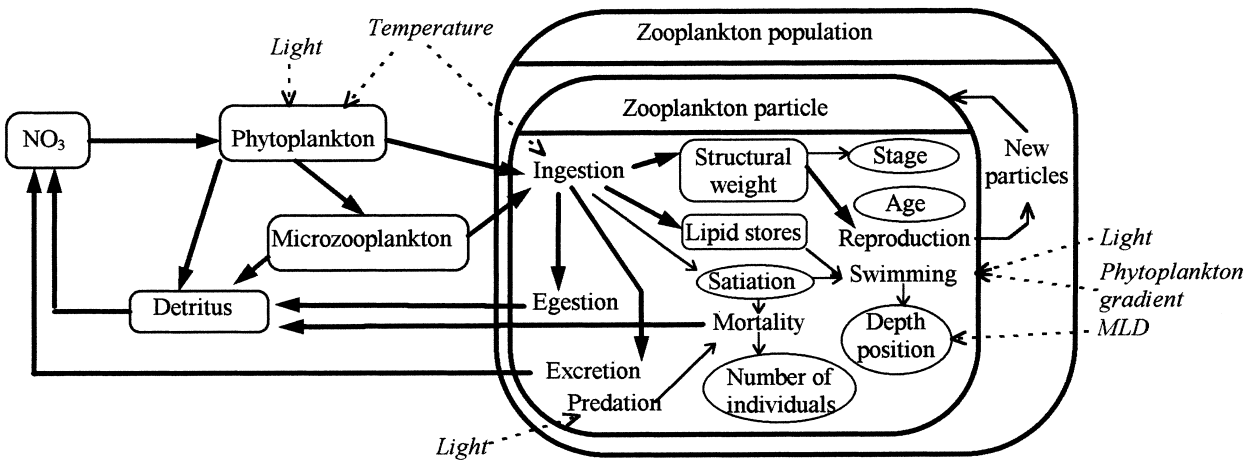

position, the number of individuals, structural weight, the lipid pool, feeding satiation level, developmental stage, age and the number of eggs produced. The processes related to the state variables are presented in Table 1.

State-variables of the particle

The depth position of the particle depends on several external and internal factors. In principle, a particle can be vertically displaced by turbulent mixing above a depth equal to 90% of the MLD. Under this depth, animals can sink passively (eggs), or can actively swim. Particles 'trapped' in the turbulent mixed layer are randomly displaced over the whole MLD during a time-step because convective overturning in the ML is shorter (≈ 20–30 min, Denman and Gargett, 1983) than the model time-step of 1 h. Only at the bottom of the mixed layer (a thin layer equal to 10% of the MLD) do particles have a chance to 'escape' by sinking or swimming.

The initial number of individuals in each particle is defined by the number of eggs produced in one night in a given layer. Females spawn their eggs once a day at noon. The number decreases due to exposure to light representing loss to visually orientating predators and natural mortality. The minimum number of individuals in a particle is 1 and if more than 600 eggs are spawned in a layer, proportionally more particles are created. The eggs produced in a given layer are supposed to be similar (i.e. we do not consider that egg quality has a major effect on future development). The initial values of characteristic variables in a particle are: the stage 'egg' and the age 'zero', the depth of creation, a fixed structural weight plus a fixed content of the lipid pool and a constant level of feeding satiation.

Growth of structural weight and filling content of the lipid pool depends on the ingested food. The structural weight of the animals has the same C/N ratio as phytoplankton and microzooplankton, but the lipid pool is assumed to be nitrogen free. Thus, nitrogen is excreted when lipids are built and the total individual C/N ratio can change due to the ratio of structural weight and lipids. The lipid pool represents the long-term nutritional history. The feeding satiation level is an index of the recent individual feeding history and is calculated as the running mean of ingestion. Since the part of mortality due to visual predators depends on body length, we relate the length to structural weight in carbon by the relationship established by Fransz and Diel (1985).

We consider 15 different stages: the nonfeeding stages and eggs are represented by the stage 'egg', following are the naupliar stages 'N3', 'N4', 'N5', 'N6', then the copepodite stages 'C1', 'C2', 'C3', 'C4', 'C5' and finally the adult stage 'Ad'. Moreover, we consider that at the moment of molting in stages C4 and C5, a proportion of individuals molt in stages called pre-overwintering C4 and C5 ('PreOSC4' and 'PreOSC5') during which the assimilated matter is only used to increase the lipid content. When the lipid content reaches a maximum value, the stage becomes overwintering 'OSC4' or 'OSC5'. The age of a particle, i.e. the age of the individuals in the particle, is incremented by time. The number of eggs produced by the females in a cohort is integrated over time for each particle, and is constrained to be less than 800 eggs/female. When this critical value is reached for a Lagrangian particle, the remaining individuals of this cohort 'die'.

Release of particles

The destruction of a particle leads to disappearance of all the individuals in the particle simultaneously. It will occur if (i) the number of individuals in the particle is below one individual/particle, (ii) the individual weight decreases below a minimal stage-related value, and (iii) for adult particles: if the accumulated number of eggs per females reaches 800 eggs. The total nitrogen of structural weight of a cancelled particle contributes to detritus.

Processes and parameter values for the 'egg' stage

The initial structural weight of the spawned eggs is set to 0.23 μg C. We consider that one half is lipids (pure carbon) and the other half represents structural weight with a constant C/N ratio. The animals do not feed at this stage and first use the lipid reserves for metabolism. Eggs and nauplii are not able to swim but sink at a constant rate. They are either 'trapped' by turbulent mixing in the ML or sink to deeper layers. The embryonic development (eggs to N2) depends on the actual temperature and time, following the function established by McLaren (1978). Because temperature varies depending on the trajectory of the particle, at each time-step, we integrate a portion of the complete development time for the particular temperature encountered (see Miller and Tande, 1993 for details). Mortality of eggs follows the same principles as for the nauplii and adults.

Biological processes from N3 to adult stages

All individuals in stages N3 to adult swim, feed, have metabolic expenditures and grow. A constant portion of adults are females and produce eggs. If animals are not trapped in the ML they swim actively. The direction depends on the underwater

light field and the level of feeding satiation. When in a good physiological state, i.e. when the indices of feeding satiation and the ratio lipid: structural weight are higher than given threshold values, copepods try to follow a given isolume which depends on the size of the animal. The maximum swimming speed depends on animal weight and on food concentration. If food concentration increases, swimming speed decreases and becomes zero when the optimal feeding rate is reached. At dawn, when a cohort starts searching for food in the upper layers and it experiences a gradient of food concentration decreasing over more than two depth layers, it will turn around and feed on the local maximum of food. If the physiological state is bad, i.e. one of the previous conditions is not fulfilled, the copepods increasingly disregard light, thus risking predation. We represent predation by a combined light-and size-dependent mortality. A constant factor is also needed to represent natural mortality and loss to non visually orientating predators.

Ingestion follows the equation presented in Table 1**.** During each one hour time-step, as a particle passes through the depth layers, food is ingested proportionally in each layer. The assimilated matter is considered to be a constant portion of ingested matter, the difference representing faecal pellets which are immediately transferred to the detritus pool. Metabolic expenditure is divided into two components: basic and active metabolism. If metabolic losses exceed the assimilated carbon these are taken from the lipid stores. When no lipids remain, the metabolic requirements are taken from the structural weight. In this case the loss in nitrogen has to be balanced by adding it to the nutrient pool. The structural weight of an animal may decrease until a stage-dependent minimum weight is reached, and then the particle is released. Moulting to the next stage occurs when 'critical moulting weight' is reached. During the molting process a small portion of the structural weight is lost and is balanced by detritus.

Egg production, related to a proportion of the population defined by a sex ratio term (f/f + m), only occurs if the average weight of the animals reaches the structural weight. Subsequently, net ingestion and a portion of stored lipids is used to produce eggs. If the lipid pool content is less than the ingested matter then the lipid pool limits egg production.

Biological processes for pre-overwintering and overwintering stages

When stages C4 and C5 have reached the critical moulting weight, a proportion moult in the pre-overwintering stages C4 and C5. The proportion varies randomly from 30% before Day 210 to 50% thereafter. In pre-overwintering stages C4 and C5, the animals follow the same physiological and behavioural rules as C4 and C5, except that the entire assimilated matter fills the lipid reserves to a maximum value depending on stage. After that, moulting to the overwintering stage occurs. The cohorts then swim to below the permanent thermocline and remain there at a depth of between 350 and 750 m until the following spring.

Additional respiration losses due to migration are neglected. The overwintering individuals do not feed. Respiration losses, which are proportional to the structural weight to the power 0.8, are taken from the lipid pool, and if this is empty then from the structural weight. Mortality follows the same rules as for the other stages.

In spring the ascent of the overwintering individuals begins at Day 95. Because the particles representing the overwintering population are randomly distributed between 750 and 350 m depth and their ascent speed depends on their structural weight, the cohorts arrive progressively in the ML, where moulting to C4 and C5 takes place.

SIMULATIONS

Initial conditions

The initial profiles of inorganic nitrogen, phytoplankton, microzooplankton and detritus are constant with depth (equal to 10, 0.3, 0.5 and 0.8 mmol N m^{-3}, respectively). The simulation starts with 400 Lagrangian particles, randomly distributed between 350 and 750 m depth (see Fig. 3 of Longhurst and Williams, 1992). Each particle comprises 5 individuals in overwintering stage C5, with a structural weight of 120 μg C, a lipid pool of 100 μg C and an initial feeding satiation set to zero.

Ecosystem dynamics

The simulated seasonal variations in profiles of inorganic nitrogen, phytoplankton, microzooplankton and detritus are shown in Fig. 5. The depletion of nutrients at the surface (Fig. 5a) occurs during the second half of May after the MLD becomes shallower and thus the Sverdrup condition for a spring bloom has been fulfilled. The duration of the phytoplankton bloom (Fig. 5b) has a short and strong peak around 20 May. Microzooplankton grazing limits the phytoplankton bloom (Fig. 5c) which maintains a direct nutrient recycling for a while in the surface layer. It also limits sedimentation of detritus as the flux of phytoplankton to detritus has been reduced significantly (Fig. 5d). After the phytoplankton bloom, the microzooplankton

Table 1. Processes in a Lagrangian particle.

a. Particle at the stage "egg"

Relative age in the embryonic developmental duration: if $\mathrm{dev}_{\mathrm{PART}}(t) > 1$, molting in N3

$$\mathrm{dev}_{\mathrm{PART}}(t+1) = \mathrm{dev}_{\mathrm{PART}}(t) + \frac{\mathrm{d}t}{\mathrm{pegg\ 1}\ ((\mathrm{T}(\mathrm{Position}_{\mathrm{PART}})-\mathrm{pegg\ 2})^{\mathrm{pegg\ 3}}}$$

Displacement of the particle

a) A particle trapped in the Mixed Layer (90% of MLD) is advected randomly in the ML
b) If not, the displacement particle depends on relative age:
if $\mathrm{dev}_{\mathrm{PART}}$ (t) < 0.33, $\mathrm{displacement}_{\mathrm{PART}}$ = direction sinkegg d*t* and direction = 1
if $\mathrm{dev}_{\mathrm{PART}}$ (t) ≥ 0.33 (corresponding to N 1 and 2)
$\mathrm{displacement}_{\mathrm{PART}}$ = direction swimmegg d*t* and direction = −1 (upward)

Mortality of individuals in the particle (as in the general case, see in b)

Changes in structural weight and lipid content

$\mathrm{respiration}_{\mathrm{PART}} = \mathrm{respegg}\ \mathrm{weight}_{\mathrm{PART}}^{\mathrm{AW}}\ (\mathrm{QR}_{10})^{\mathrm{T}(\mathrm{position}_{\mathrm{PART}})/10}$
$\mathrm{balance}_{\mathrm{PART}} = -\mathrm{respiration}_{\mathrm{PART}}$
if $\mathrm{lipid}_{\mathrm{PART}} \geq |\mathrm{balance}_{\mathrm{PART}}|$ $\mathrm{lipidflux}_{\mathrm{PART}} = \mathrm{balance}_{\mathrm{PART}}$
if $\mathrm{lipid}_{\mathrm{PART}} < |\mathrm{balance}_{\mathrm{PART}}|$ $\mathrm{growth}_{\mathrm{PART}} = \mathrm{balance}_{\mathrm{PART}}$ and $\mathrm{excretion}_{\mathrm{PART}} = \frac{N}{C}\ \mathrm{respiration}_{\mathrm{PART}}$

b. Stages N3—N6, copepodites, adult, and pre-overwintering C4 and C5

Displacement of the particle:
a) A particle trapped in the Mixed Layer (90% of MLD) is advected randomly in the ML
b) If not, the movement of the particle is due to its swimming:
$\mathrm{displacement}_{\mathrm{PART}}$ = direction $\mathrm{swimmingspeed}_{\mathrm{PART}}$ d*t*

case 1 if the radiation ≥ tlight depending on the individual size and (a) if $\mathrm{sat}_{\mathrm{PART}}$ (t) > tsat
or (b) if $\mathrm{lipid}_{\mathrm{PART}}$ (*t*) /$\mathrm{weight}_{\mathrm{PART}}$ (*t*) > tlip direction = 1 (downward)

$$\mathrm{swimmingspeed}_{\mathrm{PART}} = \mathrm{smax}\left(\frac{\mathrm{weight}_{\mathrm{PART}}^{\mathrm{AW}}+0.2}{\mathrm{wmax}^{\mathrm{AW}}+0.2}\right) \text{and tlight= } \mathrm{refrad}\left(\frac{\mathrm{weight}_{\mathrm{PART}}^{\mathrm{AW}}}{\mathrm{wmax}^{\mathrm{AW}}}\right)^2$$

case 2 what is not occuring in case 1: $\mathrm{direction}_{\mathrm{PART}} = -1$ (upward)
(except if the food concentration in the two layers under $\mathrm{position}_{\mathrm{PART}}$ (t) is greater than the food concentration at the present position, then $\mathrm{direction}_{\mathrm{PART}} = -1$)

$$\mathrm{swimmingspeed}_{\mathrm{PART}} = \mathrm{smax}\left(\frac{\mathrm{weight}_{\mathrm{PART}}^{\mathrm{AW}}+0.2}{\mathrm{wmax}^{\mathrm{AW}}+0.2}\right) \min\left(1, \max\left(0, \frac{\mathrm{PHY(z)\ +\ MZ(z)\text{-}fmin}}{\mathrm{fmax\text{-}fmin}}\right)\right)$$

Mortality of individuals in the particle

$$\mathrm{mortality}_{\mathrm{PART}} = \mathrm{ind}_{\mathrm{PART}}\ \mathrm{mort}\left(1 + \mathrm{length}_{\mathrm{PART}} \frac{\mathrm{radiation}(\mathrm{position}_{\mathrm{PART}})}{\mathrm{radiation}\ (\mathrm{position}_{\mathrm{PART}})+\mathrm{cradiation}}\right)$$

$$\mathrm{length}_{\mathrm{PART}} = \mathrm{cm1}\ \mathrm{weight}_{\mathrm{PART}}^{\mathrm{cm2}}$$

Changes in structural weight and lipid content

$$\mathrm{ingestion}_{\mathrm{PART}} = \sum_{\mathrm{position}_{\mathrm{PART}}(\mathrm{t})}^{\mathrm{position}_{\mathrm{PART}}(\mathrm{t+1})} (\mathrm{grazing}_{\mathrm{PART}}(z) + \mathrm{predation}_{\mathrm{PART}}(z)) \left(\frac{\mathrm{d}t}{\mathrm{position}_{\mathrm{PART}(t+1)} - \mathrm{position}_{\mathrm{PART}(t)}}\right)$$

$$\mathrm{grazing}_{\mathrm{PART}}(z) = \mathrm{imax}(\mathrm{Q}_{10})^{\mathrm{T}/10}(\mathrm{weight}_{\mathrm{PART}})^{\mathrm{AW}} \min\left(1, \frac{\max(\mathrm{PHY}-\mathrm{tphy}, 0)}{\mathrm{fmax}}\right)$$

$$\mathrm{predation}_{\mathrm{PART}}(z) = \mathrm{imax}(\mathrm{Q}_{10})^{\mathrm{T}/10}(\mathrm{weight}_{\mathrm{PART}})^{\mathrm{AW}} \min\left(1, \frac{\max(\mathrm{PHY} - \mathrm{tphy} + \mathrm{MZ} - tmz, 0)}{\mathrm{fmax}}\right) - \mathrm{grazing}_{\mathrm{PART}}(z)$$

$$\mathrm{egestion}_{\mathrm{PART}} = \lambda\ \mathrm{ingestion}_{\mathrm{PART}}$$

$$\mathrm{respiration}_{\mathrm{PART}} = \left(\mathrm{resp1}(\mathrm{weight}_{\mathrm{PART}})^{\mathrm{AW}}(\mathrm{QR}_{10})^{\mathrm{MTemp}/10}\right) + (\mathrm{resp2}\ \mathrm{ingestion}_{\mathrm{PART}})$$

$$\mathrm{balance}_{\mathrm{PART}} = \mathrm{ingestion}_{\mathrm{PART}} - \mathrm{egestion}_{\mathrm{PART}} - \mathrm{respiration}_{\mathrm{PART}}$$

Table 1. (*Continued*)

if $\text{balance}_{\text{PART}} > 0$:
  $\text{growth}_{\text{PART}}$ = alpha $\text{balance}_{\text{PART}}$ (for pre-overwintering, alpha = 0)
  $\text{lipidflux}_{\text{PART}}$ = (1−alpha) $\text{balance}_{\text{PART}}$ and $\text{excretion}_{\text{PART}} = \frac{N}{C}\ \text{lipidflux}_{\text{PART}}$
if $\text{balance}_{\text{PART}} \leq 0$:
  if $\text{lipid}_{\text{PART}} \geq |\text{balance}_{\text{PART}}|$ $\text{lipidflux}_{\text{PART}} = \text{balance}_{\text{PART}}$
  if $\text{lipid}_{\text{PART}} < |\text{balance}_{\text{PART}}|$ $\text{growth}_{\text{PART}} = \text{balance}_{\text{PART}}$
and $\text{excretion}_{\text{PART}}\ \frac{N}{C}|\text{balance}_{\text{PART}}|$

Changes in feeding satiation

$$\text{sat}_{\text{PART}}(t+1) = \text{sat}_{\text{PART}}(t) + \text{dm}\left(\left(\frac{\text{ingestion}_{\text{PART}} - \text{egestion}_{\text{PART}}}{\text{weight}_{\text{PART}}}\right) - \text{sat}_{\text{PART}}(t)\right)$$

Molting
  if $\text{weight}_{\text{PART}} \geq \text{critweight}(\text{stage}_{\text{PART}})$ molting occurs
    $\text{stage}_{\text{PART}} = \text{stage}_{\text{PART}} + 1$ and $\text{weight}_{\text{PART}}$ = (1−rloss) $\text{weight}_{\text{PART}}$
  for pre-overwintering C4: if $\text{lipid}_{\text{PART}} \geq$ owlipidC4, molting in overwintering C4
  for pre-overwintering C5: if $\text{lipid}_{\text{PART}} \geq$ owlipidC5, molting in overwintering C5

Egg production occurs at midnight.
When the female weight > cmat: sw = $\text{weight}_{\text{PART}}$ − cmat
  if the lipid pool is larger than sw, the spawning is limited by proteins: surplus = 2 sw
  if the lipid pool is smaller than sw, the spawning is limited by lipids: surplus = 2 $\text{lipid}_{\text{PART}}$

$$\text{Number of eggs/female} = \frac{\min(\text{eggmax weight}_{\text{PART}}, \text{surplus})}{\text{wegginit}+\text{lipegginit}}$$

$$\text{lipid}_{\text{PART}} = \text{lipid}_{\text{PART}} - \frac{\min(\text{eggmax weight}_{\text{PART}},\ \text{surplus})}{2}$$

$$\text{weight}_{\text{PART}} = \text{weight}_{\text{PART}} - \frac{\min(\text{eggmax weight}_{\text{PART}},\ \text{surplus})}{2}$$

c. Overwintering stages C4 and C5

Displacement of the particle:
a) A particle trapped in the Mixed Layer (90% of MLD) is advected randomly in the ML
b) If not, the movement of the particle is due to its swimming:
  case 1 after day 95, overwintering C4 and C5 stages swim up 1 meter hour^{-1}.
  case 2 new molted overwintering C4 and C5 swim down 1 meter hour^{-1} down to 350 meter deep, and then swim randomly between 350 and 750 m deep.

Mortality of individuals in the particle
  $\text{mortality}_{\text{PART}}$ = mortow (1 + cmow radiation ($\text{position}_{\text{PART}}$))

Changes in structural weight and lipid content
  $\text{respiration}_{\text{PART}}$ = respow $(\text{weight}_{\text{PART}})^{\text{AW}}$
  if $\text{lipid}_{\text{PART}} \geq \text{respiration}_{\text{PART}}$ $\text{lipidflux}_{\text{PART}} = \text{respiration}_{\text{PART}}$
  if $\text{lipid}_{\text{PART}} < \text{respiration}_{\text{PART}}$ $\text{growth}_{\text{PART}} = \text{respiration}_{\text{PART}}$ and $\text{excretion}_{\text{PART}} = \frac{N}{C}\ \text{growth}_{\text{PART}}$

Molting in active C4 and C5 when overwintering C4 and C5 arrive in the upper 40 meters

concentrations slowly decrease, which permits a higher phytoplankton stock and primary production on regenerated nutrients in July, with a small peak at the very end of July. This summer production induces a period of increased detritus sedimentation and a new development of microzoplankton. In June and July detritus is mainly formed by faecal pellets and dead bodies of microzooplankton and C. *finmarchicus*, but in lower concentrations than in May and at the end of July. In September, phytoplankton, microzooplankton and detritus, all decline slowly ending up with extremely low concentrations in October.

The vertical profiles of the simulated biomass and numbers of C. *finmarchicus* based on daily profiles at midnight are presented in Fig. 6. The temporal distributions of all developmental stages are shown in Fig. 7(a) with the depth-integrated and stage-cumulative abundances. The depth-integrated biomass with

Table 2. Parameter values of the Lagrangian model of *Calanus* (wd: without dimension).

General	Q_{10} :	2.1 wd
	QR_{10} :	3.4 wd
	AW :	0.8 wd
	C/N :	6.67 wd
Egg	wegginit :	0.115 μg C
	weggmin :	0.050 μg C
	lipegginit :	0.115 μg C
	pegg1 :	2073 wd
	pegg2 :	−10.60 wd
	pegg3 :	−2.05 wd
	sinkegg :	6 m day^{-1}
	swimmegg :	3 m day^{-1}
	mortegg :	0.15 day^{-1}
	respegg :	0.01 day^{-1}
N3 to adults	smax :	1200 m day^{-1}
	wmax :	100 μg C
	tsat :	0.10 wd
	tlip :	0.10 μg C
	imax :	0.860 day^{-1}
	refrad :	0.10 watt
	fmax :	100 mg C m^{-3}
	fmin :	40 mg C m^{-3}
	tphy :	40 mg C m^{-3}
	tmz :	10 mg C m^{-3}
	λ :	0.30 wd
	resp1 :	0.01 day^{-1}
	resp2 :	0.20 wd
	alpha :	0.8 wd
	mort :	0.05 day^{-1}
	rloss :	0.10 μg C
	dm :	12 wd
	cm1 :	0.70 mm μg C^{-1}
	cm2 :	0.278 wd
	minweightN3 :	0.05 μg C
	critweightN3 = minweightN4 :	0.20 μg C
	critweightN4 = minweightN5 :	0.30 μg C
	critweightN5 = minweightN6 :	0.45 μg C
	critweightN6 = minweightC1 :	0.75 μg C
	critweightC1 = minweightC2 :	1.10 μg C
	critweightC2 = minweightC3 :	2.50 μg C
	critweightC3 = minweightC4 :	7.00 μg C
	critweightC4 = minweightC5 :	15.0 μg C
	critweightC5 = minweightAd :	40.0 μg C
	critweightad :	90 μg C
	cmat :	100 μg C
Overwintering C4 and C5:	owlipC4 :	100 μg C
	owlipC5 :	100 μg C
	respow :	0.001 day^{-1}
	mortow :	0.001 day^{-1}
	cmow :	0.0025 $watt^{-1}$

a separation of biomass above and below 300 m depth is given in Fig. 7(b). After Day 95, the population of overwintering *Calanus* copepodites migrates towards the surface. Due to their different vertical position at the beginning of the ontogenic migration, the arrival of the population in the surface layer extends over a few weeks in April. The main biomass of *Calanus* is then found in the upper layer, where molting in active C5 and adults takes place. These stages then induce the development of a first generation in the first half of May, with high densities of individuals evenly distributed above the MLD (Fig. 6a). The total abundance of nauplii reaches 120 000 individuals m^{-2} in mid-May (Fig. 7a). The integrated abundance of eggs, and N1 and N2 stages, shows two peaks, the first around 7 May occurring before the bloom and a second peak coinciding with the bloom itself, around 20 May. The first peak corresponds to an egg production mainly based on the lipid reserves and on feeding on low food concentrations. At the beginning of June, copepodites and adult abundances of this first generation reach 50 000 individuals m^{-2} which leads to a peak in biomass of roughly 1 g C m^{-2} (Fig. 7b). During the night, the copepodites and adults are concentrated in layers around the MLD (Fig. 6a).

During the second half of June the population of copepodites is divided into two groups, a part of the population enters the overwintering state and migrates to deeper layers while the other part continues to grow and initiates the second generation. The migration of overwintering copepodites is not visible in terms of abundance (which is too low), but the presence of copepods is shown by low biomass concentrations between 100 and 300 m depth. The integrated biomass of animals below 300 m depth (i.e. overwintering copepodites) increases up to 200 mg C m^{-2} between 20 June and 20 July (Fig. 7b).

The second generation of *Calanus* develops from 20 June to the beginning of August (Figs. 6 and 7). The production of eggs is slightly higher for the second generation than for the first (Fig. 7a), and the highest depth integrated number of eggs is around 130 000 individuals m^{-2} in mid-July. The total *Calanus* biomass in the upper layer reaches 1.6 g C m^{-2}. This biomass peak induces a grazing pressure on microzooplankton, which allows phytoplankton to re-develop in the euphotic zone (Figs. 5b and c). At the end of July, a second wave of overwintering copepods migrates to deeper layers, visible in terms of biomass (Fig. 6b). Considering the biomass of individuals below 300 m depth (Fig. 7b), the recruitment of overwintering individuals from the second generation is shorter (5–20 August) than the first, but similar in terms of integrated biomass. The highest biomass of overwintering animals is around 450 mg C m^{-2} at the end of August, whereas the highest integrated abundance is 5000 individuals m^{-2} in September. Some individuals which continue development into adults, spawn eggs in August, but the development of this third generation has stopped during the second half of August.

Figure 5. Simulated profiles at Station India of (a) nutrients, (b) phytoplankton, (c) microzooplankton and (d) detritus.

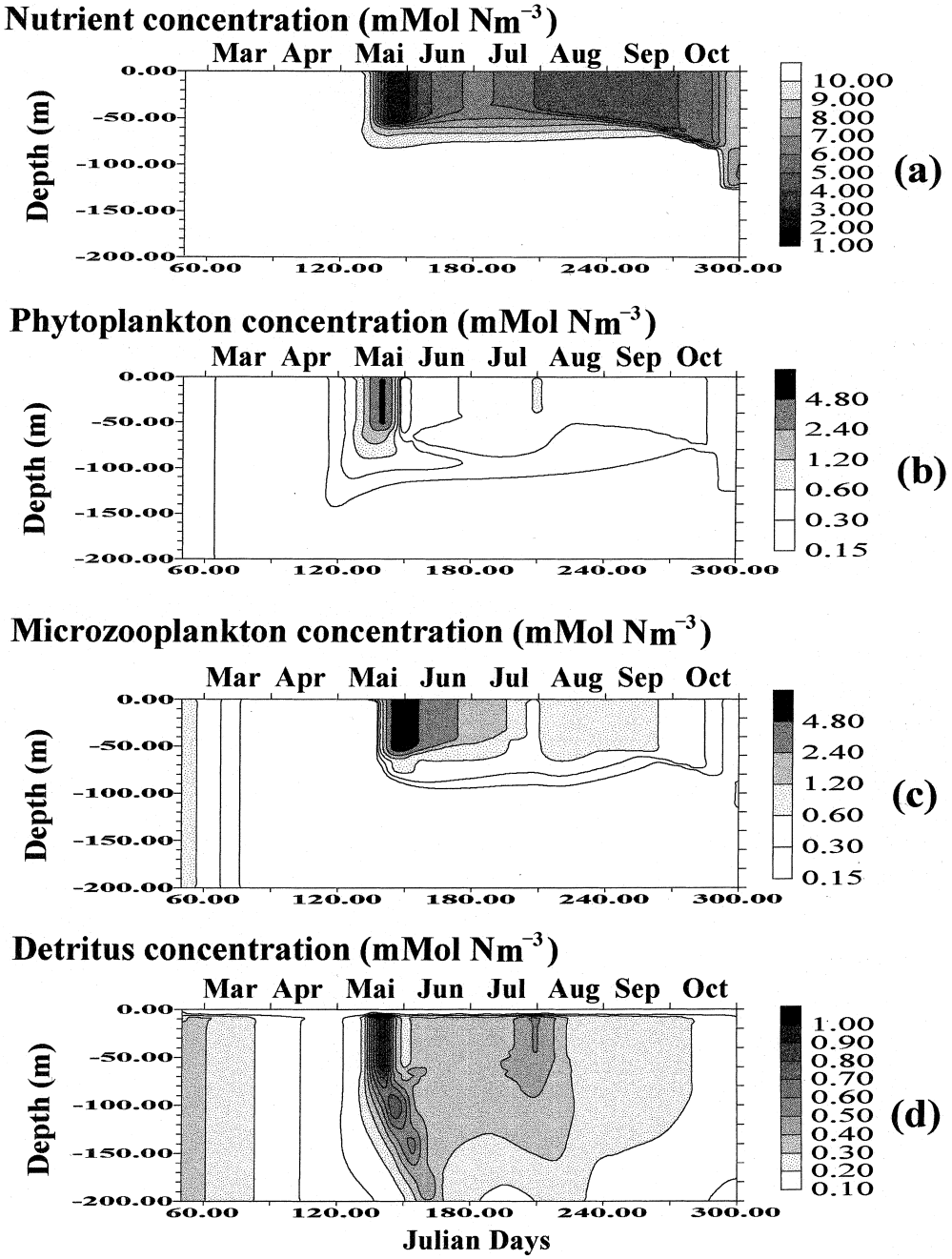

Life history of isolated particles

The trajectories of four particles during different periods of the year are presented in Fig. 8. The particles, created at the beginning of the simulation (red), move randomly between depths of 350 and 750 m. All particles begin to swim up at day 95, and arrive progressively in the upper 40 m between Days 115 and 140 (25 April – 20 May). Overwintering copepods moult to active copepodites in the upper layers, and then resume growth and spawn eggs at the adult stage. The newly created particles (green) appear after Day 130 (Fig. 8). They are initially confined to the mixed layer but later are restricted to below the MLD. At a finer scale of resolution, particles can be seen to un-

Figure 6. Simulated profiles at Station India of (a) biomass and (b) numerical abundance of *Calanus*.

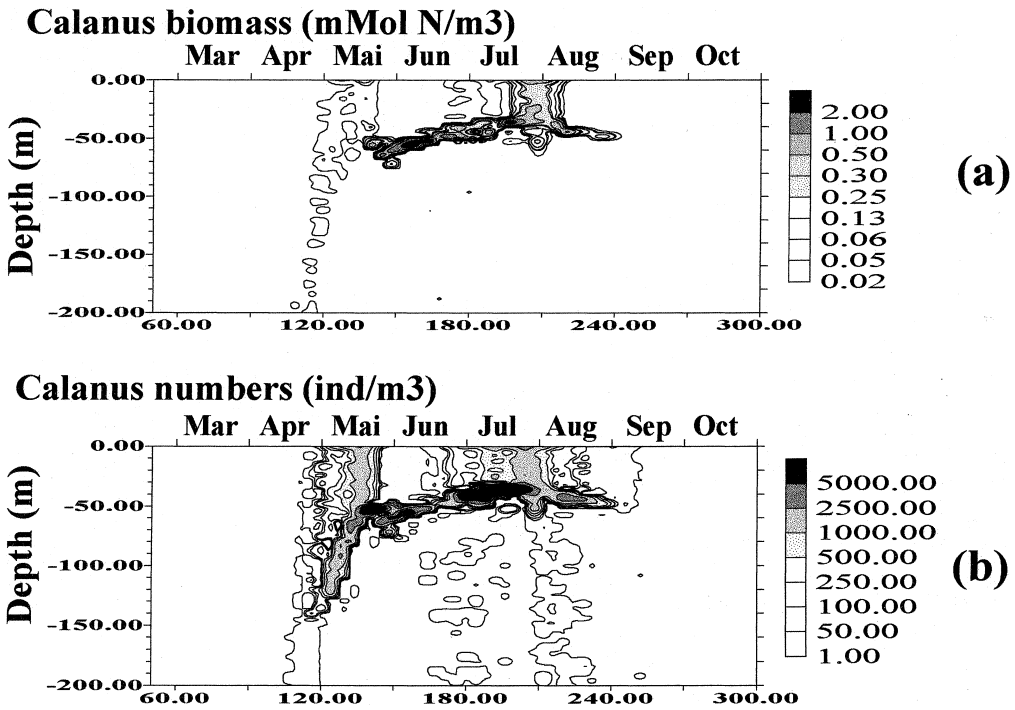

Figure 7. Simulated results showing (a) vertically integrated cumulative abundance of egg to N2, N3 to N6, copepodites and adults, and overwintering copepodites; (b) vertically integrated *Calanus* biomass above and below 300 m depth.

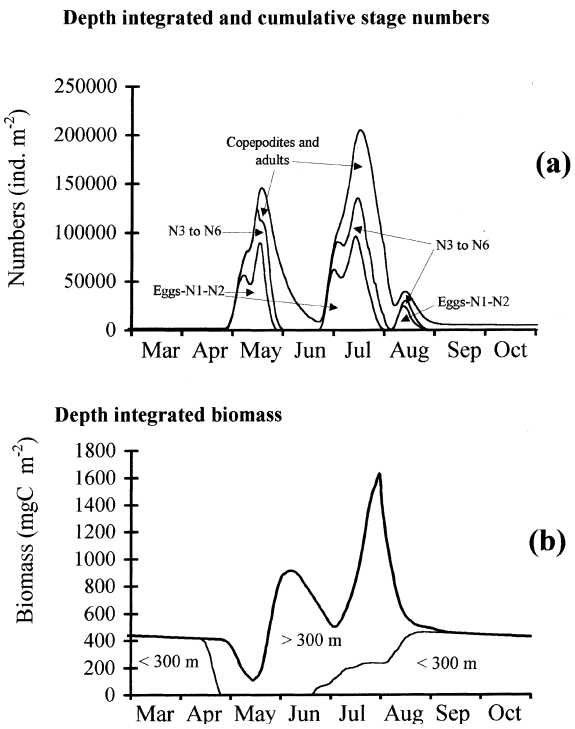

dertake vertical nycthemeral migrations (Figs. 9a and b). As the animals grow, they are obliged to swim deeper to avoid predators as light tolerance decreases with body length, while swimming speed increases with weight. Two of the four particles shown in Fig. 8 swim to deeper layers after day 180 to overwinter. The precocious one (yellow) overwinters at the C4 stage. The second particle (green) is an overwintering C5, and swims down 10 days after the first one.

The two last particles of the first generation represented in Fig. 8 continue to grow into the adult stage, spawn and die (Days 190 and 205). The hourly resolved trajectory of this second particle is presented in Fig. 9(b). The depth of diurnal migration increases continuously, with a greatest depth of more than 300 m (adult). In July, when the MLD is shallow and food abundance is low, animals explore the shallowest layers and occasionally stay trapped in the mixed layer for some time, which leads to incomplete migration during those days. At Day 190, a new particle (in black) is created which belongs to the second generation. Experiencing the highest temperatures, its development time is short, and it migrates to deep water as an overwintering C4 in early August (Fig. 9b).

Figure 10 shows the survival curve of the four partices created in May (Fig. 8). Three of them, created in layers of high spawning activity, start with

Figure 8. Vertical trajectories based on night positions of four particles of the overwintering generation in red, of the first generation in blue and green, and of one particle of the second generation in black.

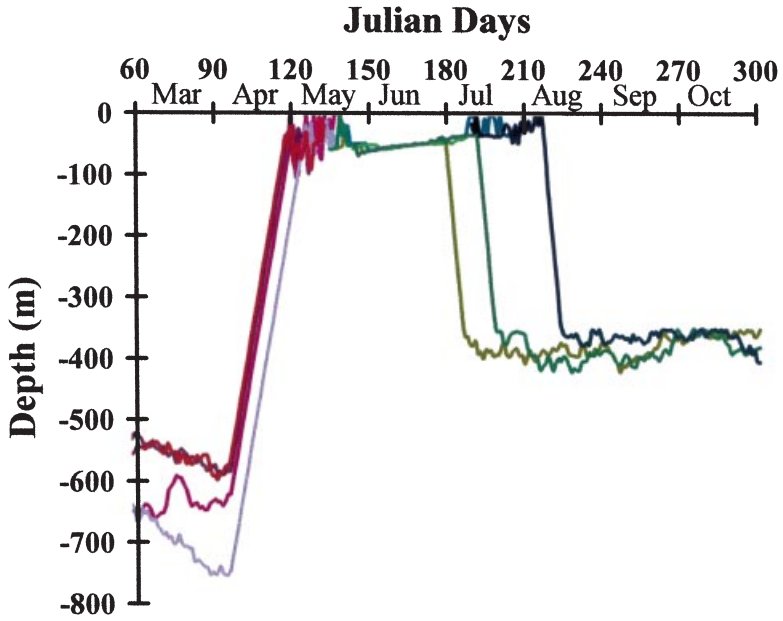

around 500 individuals. The fourth one comprises around 50 individuals. A high mortality initially occurs when the stage corresponds to eggs, N1 and N2 stages. The particle starting with 50 individuals is removed at day 187 when the number of individuals is lower than one. Individual growth of total weight (structural weight and lipids) of the four particles shows different patterns (Fig. 11). All curves show near exponential growth with short interrupts due to the loss of matter during molting. Two particles reach a total weight just above 100 μg C at C4 stage and with a large lipid content. One dies at Day 187 while the other overwinters. One other particle overwinters as C5 with accumulated lipids and a total weight of 250 μg C. The remaining particle continues to grow and spawn eggs for the second generation and shows weight fluctuations towards the end of its life due to the production of clutches of eggs.

Figure 9. A finer scale plot of part of the track of two particles of the first generation (same colour for each particle as in Fig. 8).

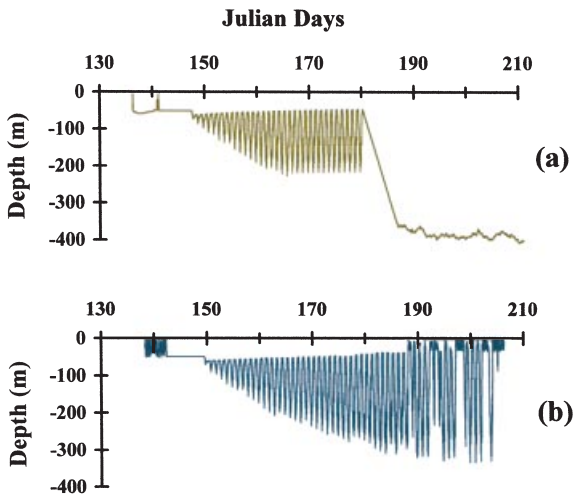

Vertical distributions

One important advantage of the model is that it allows the possibility to study processes influencing the ver-

Figure 10. Survival curves of four particles of the first generation (the same particles as in Fig. 8 with the same colours).

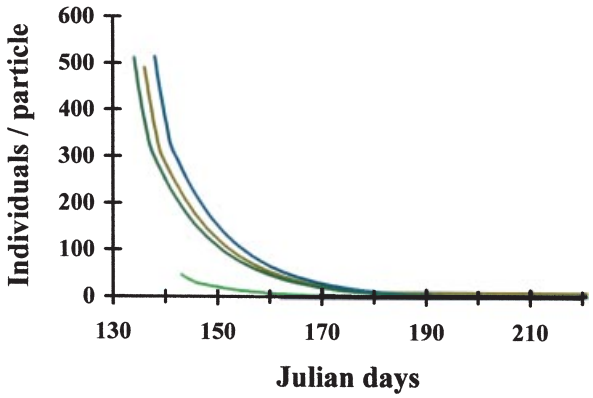

Figure 11. Total body weight of the four particles presented in Fig. 10.

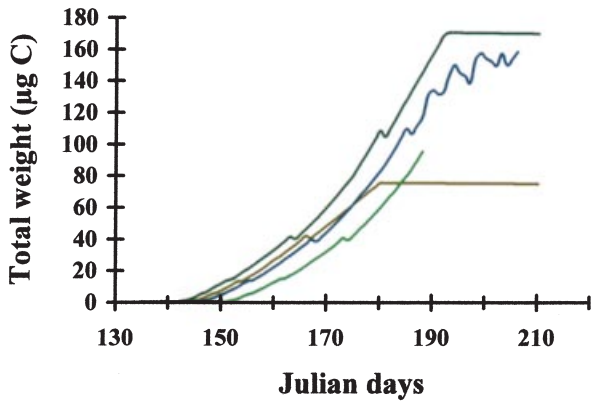

tical distribution of *Calanus* by stages. Figure 12 presents an example of distribution on day 210 (end of July), when the MLD is at 40 m depth. The vertical simulated profiles at midnight show that a large part of the population is trapped in the mixed layer or just below, except for pre-overwintering C5 stages which are distributed throughout the water column. Particles just above the MLD avoid being fully mixed into the ML and hence accumulate at the base of the MLD where the food is high enough and the risk of predation during the night is reduced. Some copepodites accumulate between 40 and 60 m depth because the local phytoplankton and microzooplankton concentrations allow them to feed adequately in this depth range.

DISCUSSION

Considering the present results of the Lagrangian *Calanus* model, although the simulated isotherm profiles (Fig. 1b) were quite schematic due to our simple forcing, they were comparable in timing to those observed in 1972 (Fig. 8b of Williams, 1988), a 'typical year for this station' (Williams, 1988). The observed peak of chlorophyll *a* in 1972 occurred on 14 May, and reached 207.6 mg Chl a m^{-2}, evenly distributed through the upper 80 m (Fig. 5b of Williams, 1988). Our simulated bloom is slightly delayed (around 1 week) relative to the observation, a result also obtained by Fasham (1993, his Fig. 10). In the simulation, there was also a delayed nutrient depletion after the bloom and rather too high a peak of phytoplankton concentrations (3 mg Chl a m^{-3}) in comparison with the field data (Fasham, 1993). Moreover, two further blooms (around 2 mg Chl a m^{-3}) occurred at the beginning of July and September in 1972 (Fig. 7b of Williams, 1988 and Fig. 10 of Fasham, 1993), which are not reproduced by our model. Although observational data for microzooplankton and small copepods are not available from Station India, our simulated values seem to be too high compared with concentrations recorded from the position 47°N, 18°W (Verity *et al.*, 1993). However, bearing in mind that the model has not been optimized to the field data the simulated ecosystem seems still to provide a plausible environment for our *Calanus* model.

The simulated population dynamics of *Calanus* presents two complete generations and the beginning of a third one. The two first generations are quite distinct, the first occurring in the spring and the other in the summer (Fig. 7a). The main features of the population dynamics and vertical distributions of *Calanus* simulated with our model (Fig. 6) correspond well with the observations of Williams (1988, his Fig. 4b) and by Longhurst and Williams (1992). Williams (1988) presents distributions of copepodite numbers whereas our results for numerical abundances represent all stages (eggs, nauplii and copepodites; Fig. 6a). However, the simulated biomass distributions (Fig. 6b), which are mainly composed of copepodites, give comparable distributions to those of Williams (1988). The total integrated abundance obtained with our simulations are around 10 times higher than those given by Williams (1988, his Fig. 4b) even considering that the data of Williams (1988) includes counts of copepodites only. Our highest simulated concentrations of copepodites are above 50 000 individuals m^{-2}, such densities are not unrealistic having occurred at Station India in 1973 (Fig. 5b of Williams, 1988) and higher concentrations having been observed elsewhere (Sameoto and Herman, 1990). However, our simulated biomass of *Calanus* seems to be regularly higher throughout the year than that presented by Longhurst and Williams (1992, their Fig. 2), although net sampling tends to underestimate abundances.

The highest simulated concentrations of *Calanus* were located in layers between 30 and 60 m depth in May and in June–July, just under the MLD. The parameterization of the swimming process in our model provides the copepods with a tendency to concentrate at the deepest layer where food is adequate, depending on development stage. Longhurst and Williams (1979) also mentioned possible differences in the depth distribution of different stages of *Calanus finmarchicus*. Our simulated distribution in August (Fig. 12c) appears very similar to those obtained in August by Longhurst and Williams (1979, their Fig. 5a). In both simulated and observed distributions, the peak of stage abundance was situated at 30–40 m depth, probably near the MLD. Vertical profiles of *Calanus* stages often show different vertical distribution patterns following

Figure 12. Vertical distributions at midnight on Day 210 of phytoplankton, microzooplankton and developmental stages of *Calanus*.

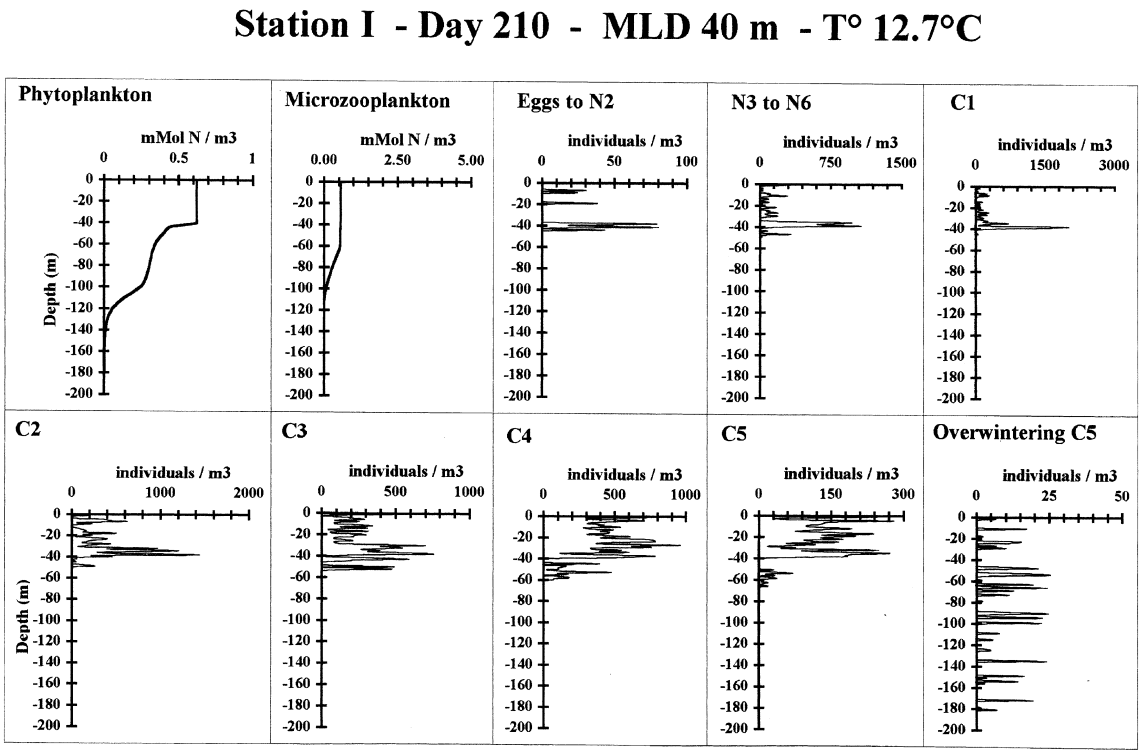

the degree of mixing or stratification of the water column. A consequence of the vertical structuring is that grazing pressure on phytoplankton and microzooplankton is not evenly spread through the mixed layer, but is mainly where the larger grazers are present.

Individual trajectories show vertical migration varying with both external and internal factors. The deeper depth limit of the daily migration increases with developmental stage: this feature was also proposed by Krause and Radach (1989) from analysis of depth profiles from FLEX data. However, the amplitude of the migration in FLEX was less (since the North Sea is shallower than at Station India). The other aspects influencing migration (light, trapping in the mixed layer, relation to prey profiles, feeding satiation and lipid content) all require investigation in further model experiments.

Figure 13. Variability in the number of Lagrangian particles by development stage during the simulation.

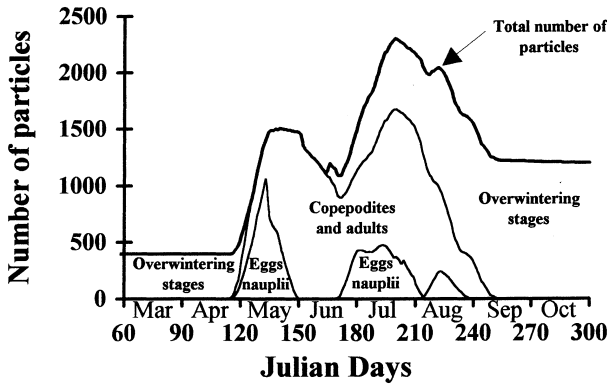

The number of modelled particles and the number of individuals represented by each particle are two important aspects of our model. Figure 13 shows the temporal variation in numbers of Lagrangian particles required during the standard run with a maximum of roughly 2000 particles at the end of July. At the end of June, when the second generation starts, there are still around 1000 particles left, whereas the total number of individuals per particle is extremely low (around 10 individuals per particle). Production of the second generation leads to the creation of more than 1000 new particles. At the end of July the number of particles decreases significantly because those down to 1 individual per particle are 'killed' off. During the growth and reproductive seasons the number of Lagrangian particles stays above 20 m^{-2} in the ML, which guarantees statistical significance of the results (Wolf, 1991).

The presented model is a step forward for coupling Lagrangian models of zooplankton with their environment. We choose Station India for the simulation and following Longhurst and Williams (1992), we made the assumption that mesoscale activity and advection do not strongly affect the seasonal change of *Calanus* at this location. In future we would like to simulate the population dynamics of *Calanus finmarchicus* at different locations in the North Atlantic, including a detailed sensitivity study of our parameterizations.

ACKNOWLEDGEMENTS

F.C. wishes to thank Roger Harris and the GLOBEC committee for inviting him to the First Open Science Meeting of GLOBEC, as well as to SCOR for travel funding. Thanks are also due to an anonymous referee for critical reading and suggestions, and to Steve Coombs for his help in the editing. The work presented here was initially supported by the French–German cooperation program PROCOPE (contract 95114) in the form of travel funding, and by the French JGOFS program (CNRS/INSU) for equipment and facilities. This work is also a contribution to the Trans-Atlantic Study of *Calanus finmarchicus* as F.C. obtained a support from the commission of the European Community under contract MAS3-CT95–0039 (TASC) of the MAST III Programme to continue this work.

REFERENCES

Barkmann, W. and Woods, J.D. (1996) On using a Lagrangian model to calibrate primary production determined from in vitro incubation measurements. *J. Plankton Res.* **18:**767–788.

Batchelder, H.P. and Miller, C.B. (1989) Life history and population dynamics of *Metridia pacifica*: results from simulation modelling. *Ecol. Mod.* **48:**119–136.

Batchelder, H.P. and Williams, R. (1995) Individual-based modelling of the population dynamics of *Metridia lucens* in the North Atlantic. *ICES J. Mar Sci.* **52:**469–482.

Carlotti, F. and Radach, G. (1996) Seasonal dynamics of phytoplankton and *Calanus finmarchicus* in the North Sea as revealed by a coupled one-dimensional model. *Limnol. Oceanogr.* **41:**522–539.

DeAngelis, D.L. and Gross, L.J. (1992) *Individual-Based Models and Approaches in Ecology*. New York: Chapman and Hall, 525 pp.

Denman, K.L. and Gargett, A.E. (1983) Time and space scales of vertical mixing and advection of phytoplankton in the upper ocean. *Limnol. Oceanogr.* **28:**801–815.

Fasham, M., Ducklow, H. and McKelvie, S. (1990) A nitrogen-based model of plankton dynamics in the oceanic mixed layer. *J. Mar. Res.* **48:**591–639.

Fasham, M.J.R. (1993) Modelling the marine biota. In: *The Global Carbon Cycle*. M. Heimann (ed.). NATO ASI Series, Vol. I 15, Berlin: Springer-Verlag, pp. 457–504.

Fasham, M.J.R., Sarmiento, J.L., Slayter, R.D., Ducklow, H.W. and Williams, R. (1993) Ecosystem behavior at Bermuda station S and ocean weather station India: a general circulation model and observational analysis. *Global Biogeochem. Cycles* **7:**379–415.

Fransz, H.G. and Diel, S. (1985) Secondary production of *Calanus finmarchicus* (Copepoda: Calanoidea) in a transitional system of the Fladen Ground area (northern North Sea) during the spring of 1983. In: *Proceedings of the 19th European Marine Biology Symposium*. P.E. Gibbs (ed.). Cambridge, UK: Cambridge University Press, pp. 123–135.

Hinckley, S., Herman, A.J. and Megrey, B.A. (1996) Development of a spatially explicit, individual-based model of marine fish early life history. *Mar. Ecol. Prog. Ser.* **136:**47–68.

Krause, M. and Radach, G. (1989) On the relations of vertical distribution, diurnal migration and nutritional state of herbivorous zooplankton in the Northern North Sea during FLEX 1976. *Int. Rev. Ges Hydrobiol.* **74:**371–417.

Longhurst, A. and Williams, R. (1979) Materials for plankton modelling: vertical distribution of Atlantic zooplankton in summer. *J. Plankton Res.* **1:**1–28.

Longhurst, A. and Williams, R. (1992) Carbon flux by seasonal vertical migrant copepods is a small number. *J. Plankton Res.* **14:**1495–1509.

McLaren, I.A. (1978) Generation lengths of some temperate marine copepods: estimation, production and implications. *J. Fish Res. Bd Can.* **345:**1330–1342.

Miller, C.B. and Tande, K.S. (1993) Stage duration estimation for *Calanus* population, a modelling study. *Mar. Ecol.. Prog. Ser.* **102:**15–34.

Miller, C.B., Lynch, D.R., Carlotti, F., Gentleman, W. and Lewis, C.V.W. (1998) Coupling of an individual-based population dynamical model of *Calanus finmarchicus* to a circulation model for the Georges Bank region. *Fish. Oceanogr.* **7**: 219–234.

Sameoto, D. and Herman, A.W. (1990) Life cycle and distribution of *Calanus finmarchicus* in deep basins on the Nova Scotia shelf and seasonal changes in *Calanus* spp. *Mar. Ecol. Prog. Ser.* **66:**225–237.

Smith, E.L. (1936) Photosynthesis in relation to light and carbon dioxide. *Proc. Nat. Acad. Sci.* **22:**504–511.

Verdier, C., Carlotti, F., Rey, C. and Bhaud, M. (1997) A model study of the role of wind-driven currents and vertical larval behavior on the recruitment of the annelid *Owenia fusiformis* in Banyuls Bay. *Mar. Ecol. Prog. Ser.* **160:**217–231.

Verity, P.G., Stoecker, D.K., Sieracki, M.E. and Nelson, J.R. (1993) Grazing, growth and mortality of microzooplankton during the 1989 North Atlantic spring bloom at 47°N, 18°W. *Deep-Sea Res.* **40:**1793–1814.

Werner, F.E., Page, F.H., Lynch, D.R., Loder, J.W., Lough, R.G., Perry, R.I., Greenberg, D.A. and Sinclair, M.M. (1993) Influences of mean advection and simple behavior on the distribution of cod and haddock early life stages on Georges Bank. *Fish. Oceanogr.* **2:**43–64.

Williams, R. (1988) Spatial heterogeneity and niche differentiation in oceanic zooplankton. *Hydrobiologia* **167/168:**151–159.

Wolf, K.U. (1991) Meridional variability of the physical and planktological seasonal cycle – Lagrangian model-studies in the North Atlantic. *Reports Inst. Mar Sci., Kiel* **203:**119 pp.

Woods, J. and Onken, R. (1982) Diurnal variation and primary production in the ocean – preliminary results of a Lagrangian ensemble model. *J. Plankton Res.* **4:**735–756.